# Energy spectra of neutrino-induced upward muons in underground experiments

T. K. Gaisser
*Bartol Research Institute, University of Delaware, Newark, Delaware 19716*

A. F. Grillo
*INFN—Laboratori Nazionali di Frascati, P.O. Box 13, 00044 Frascati, Italy*
(Received 28 July 1986; revised manuscript received 16 July 1987)

One major goal of large underground detectors is to search for energetic neutrinos of astrophysical origin, for example, from point sources such as Cygnus X-3 or SN1987A. We investigate how the energies of the muons at the detector reflect the energies of the parent neutrinos. A measurement of the muon energy may help distinguish between a background of relatively-low-energy neutrinos of atmospheric origin and a signal from a point source if the latter has a hard neutrino spectrum, as expected in most models.

## I. INTRODUCTION

The possibility of measuring fluxes of high-energy cosmic neutrinos with underground experiments depends on detection of muons produced by charged-current interactions of neutrinos. The interaction can take place either inside a large detector or in the material surrounding the detector. In either case, one depends on the long range of the muons to extend the sensitive area of the detector and so overcome the low flux times interaction rate of the neutrinos. Upward fluxes of neutrino-induced muons have been measured[1] and are in agreement with what is expected from $\nu_\mu$ and $\bar{\nu}_\mu$ produced by cosmic-ray interactions in the atmosphere on the other side of the Earth.[1-3] Downward-going muons are of course also produced by atmospheric neutrinos, but they are overwhelmed by muons produced in the atmosphere which penetrate down to the detector.

The rate of neutrino-induced muons depends on the differential charged-current neutrino cross sections as well as on the neutrino flux and muon range. For atmospheric neutrinos, the flux is so steep ($dN_\nu/dE_\nu \propto E^{-3.7}$) that the rate of muons above several GeV at the detector practically depends only on the neutrino cross section below several hundred GeV where it has been directly measured. Possible extraterrestrial sources of neutrinos may, however, have much flatter energy spectra, in which case the behavior of the neutrino cross section at very high energy becomes more important. The same is also true if the detection threshold energy is very high, as in the case of the search at Fly's Eye[4] for upward extensive air showers induced by electron neutrinos. In this case, in addition to including the effect of the $W$ propagator in the charged-current cross section,[5] it is necessary also to take account of the QCD evolution of the structure functions, which increases the cross section significantly above the scaling limit for neutrino energies above about 100 TeV (Refs. 6–8).

McKay and Ralston[7] evaluated the effect of QCD evolution on the cross section with an analytic approximation valid for $s = 2ME_\nu \gg M_W^2$. Quigg, Reno, and

Walker[8] then made a quantitative calculation applicable at all energies. We first review the calculation of the cross section which we had made independently[9] in order to justify our use of a different set of QCD-evolved structure functions.[10] After showing that the results for the cross sections are indistinguishable from those of Ref. 8 up to neutrino energies of $10^6$ TeV, we discuss the distribution of muon energies at the detector. Our goal is to compute the muon energy spectrum at the detector quantitatively for possible use in discriminating experimentally among various parent-neutrino spectra. We conclude with a discussion of the extent to which a measurement of neutrino energies at the detector could help distinguish an astrophysical neutrino signal from atmospheric background if, as expected, the signal has a harder spectrum than the background.

## II. CROSS SECTION AND STRUCTURE FUNCTIONS

The differential charged-current neutrino cross section is given by

$$\frac{d\sigma^{\nu(\bar{\nu})}}{dx\,dy} = \frac{G_F^2 m E_\nu}{\pi} \left[ \frac{1}{1+2mE_\nu xy/M_W^2} \right]^2$$
$$\times \left[ \left[ 1-y+\frac{y^2}{2} \right] F_2 \pm \left[ y-\frac{y^2}{2} \right] xF_3 \right] , \qquad (1)$$

where $x = Q^2/2m(E_\nu - E_\mu)$ and $y = 1 - E_\mu/E_\nu$ are the usual scaling variables. The structure functions $F_i(x,Q^2)$ are expressed in terms of parton distributions on an isoscalar nucleon target. For example,

$$F_2^\nu = x(u_v + d_v + u_s + d_s + 2s + 2b + 2\bar{u} + 2\bar{c} + 2\bar{t}) , \qquad (2)$$

where $d$ and $u$ refer to the quark distributions in the proton and the subscripts $v$ and $s$ refer to valence and sea. For energies such that $s \gg M_W^2$ the cross section can, as shown in Ref. 7, be approximated by

$$\sigma \simeq \frac{M_W^2 G_F^2}{2\pi} \int_{M_W^2/s}^1 \frac{F_2(x,M_W^2)}{x} dx . \qquad (3)$$

To evaluate the cross section up to $s \gg M_W^2$ GeV, one needs the structure functions at $Q^2 \sim M_W^2$ down to $x \sim Q^2/s$. In principle, the power-law form of the $x$ dependence of the structure functions used by Duke and Owens[10] is incorrect for extrapolation below $x = 0.001$. The theoretically preferred double-logarithm approximation[11] was used in Refs. 7 and 8. In practice, however, the two procedures give the same results up to $E_\nu \sim 10^9$ GeV. According to Eq. (3) this can be seen by comparing $F_2$ evaluated at $x = M_W^2/s$ and $Q^2 = M_W^2$ as calculated in the two different ways:

$$F_2 = 0.0351 \exp\{2.45[\ln(s/M_W^2)]^{1/2}\}$$
$$\times \{[\ln(s/M_W^2)]^{1/2}\}^{-1} , \quad (4a)$$

$$F_2 = 0.449(s/M_W^2)^{0.383} + 0.121(s/M_W^2)^{0.302} . \quad (4b)$$

In the expression (4b) from Ref. 10, the first term is from the sum of up, down, and strange seas and the second from the charm contribution. Bottom and top are set to zero in Ref. 10. Equation (4a) is the form from Ref. 7. For $s \gg M_W^2$ the contribution of valence quarks can be neglected.

The numerical values for the two forms are given in Table I. The neutrino cross section as a function of energy is shown in Fig. 1. Curve (a) is the old result from Ref. 5, which is low at high energy because of the use of scaling structure functions. Curve (b) uses the QCD-evolved structure functions of Ref. 10. Curve (b) agrees within 10% with the cross section calculated in Ref. 8. The cross section of McKay and Ralston[7] is 50% low at $10^5$ GeV because of their neglect of valence quarks. Their result crosses that of Ref. 8 around $10^7$ GeV and is about 30% above it in the region from $10^9$–$10^{10}$ GeV. The two methods of incorporating QCD evolution clearly give virtually identical results up to $10^9$ GeV, which is much higher than we need for the present application. In the remainder of the paper, we will therefore use the forms of Ref. 10 to represent scaling violation.

### III. EVALUATION OF NEUTRINO-INDUCED SIGNAL

The full expression for the neutrino-induced signal is[5]

$$S(>E_\mu) = \int_{E_\mu}^\infty dE_\nu \frac{dN_\nu}{dE_\nu} P(E_\nu, E_\mu) , \quad (5)$$

where $dN_\nu/dE_\nu$ is the neutrino energy spectrum and $P(E_\nu, E_\mu)$ is the probability that a neutrino aimed at the detector gives a muon with energy above $E_\mu$ at the detector. The advantage of expressing the result in this form[5] is that it divides the signal into two factors, one of which is the neutrino flux and the other a function which depends only on neutrino cross section and muon

propagation. The latter is given by

$$P(E_\nu, E_\mu) = \int_{E_\mu}^{E_\nu} dE'_\mu \left[ \int_{E'_\mu}^{E_\nu} dE''_\mu \frac{d\sigma}{dE''_\mu} N_A \right. $$
$$\left. \times \int_0^\infty dX\, g(X, E'_\mu, E''_\mu) \right] , \quad (6)$$

where $N_A$ is Avogadro's number and $g(X, E'_\mu, E''_\mu)dE'_\mu$ is the probability (differential in $E'_\mu$) that a muon produced with energy $E''_\mu$ travels a distance $X$ (g/cm$^2$) and ends up with energy in $dE'_\mu$.

If the average energy-loss rate for muons is expressed as

$$dE/dX = -\alpha - \beta E , \quad (7)$$

then in the approximation that range straggling is neglected

$$E'_\mu = e^{-\beta X}(E''_\mu + \epsilon) - \epsilon , \quad (8)$$

where $\alpha \simeq 2$ MeV/(g/cm$^2$) and $\epsilon = \alpha/\beta \simeq 510$ GeV. The range to go from $E''_\mu$ to $E'_\mu$ is then

$$X_0 = \frac{1}{\beta} \ln \left[ \frac{E''_\mu + \epsilon}{E'_\mu + \epsilon} \right] . \quad (9)$$

In this approximation $g(X, E'_\mu, E''_\mu) \propto \delta(X - X_0)$, so the integral over the range in Eq. (6) can be done trivially.

The cross section is

$$\frac{d\sigma}{dE''_\mu} = \frac{1}{E_\nu} \int_0^1 \frac{d\sigma}{dx\,dy} dx , \quad (10)$$

where $d\sigma/dx\,dy$ is given in Eq. (1). Thus to evaluate $P(E_\nu, E_\mu)$ requires a triple integration over $x$, $y$, and $E'_\mu$. Particular care is required in handling the integration near $xy \lesssim M_W^2/2ME_\nu$, especially for flat neutrino spectra where large $E_\nu$ is important. The outer integration over $E'_\mu$ can be done by parts, leaving a double numerical integration. This was the calculation done in Ref. 5. Figure 2 shows the result of repeating this calculation with the QCD-evolved structure functions of Ref. 10 for muons with $E_\mu > 2$ GeV at the detector. QCD evolution is of practical importance here only for $E_\nu \gtrsim 10^5$ GeV. To see how the signal depends on neutrino energy for a given neutrino spectrum, one only needs to multiply $P(E_\nu, E_\mu)$ by the neutrino spectrum. The comparison with the previous result is shown in Fig. 3. One sees that QCD evolution is negligible for power-law neutrino spectra with indices greater than 2.2.

TABLE I. Numerical values for the two forms of $F_2$.

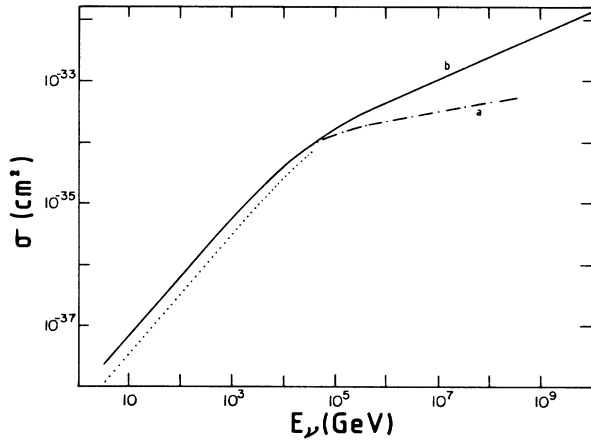| $\log_{10}[E_\nu$ (GeV)] | 5 | 6 | 7 | 8 | 9 | 10 | 11 |
|---|---|---|---|---|---|---|---|
| $F_2$ (Ref. 7) | 1.7 | 5.0 | 12.5 | 29 | 59 | 115 | 220 |
| $F_2$ (Ref. 10) | 2.0 | 4.6 | 11 | 26 | 61 | 144 | 340 |

FIG. 1. Total neutrino and antineutrino cross sections. Dotted curve refers to antineutrinos. Note that above $10^6$ GeV neutrino and antineutrino cross sections are equal. Curve (a) is obtained through the use of scaling structure functions, (b) with evolved ones.

## IV. MUON SPECTRUM AT THE DETECTOR

To see how the muon energy spectrum at the detector reflects the neutrino spectrum, it is necessary to evaluate

$$\int_{E_\mu}^{\infty} dE_v \frac{dN_v}{dE_v} \frac{dP(E_v,E_\mu)}{dE_\mu} \quad ,$$

for a range of values of $E_\mu$. Here $dP/dE_\mu$ is the integrand of Eq. (6), and one cannot use the integration by parts to simplify the calculation. Figures 4 and 5 show the results for muon spectra induced by power-law neutrino spectra with $2 \leq \gamma \leq 3.6$.
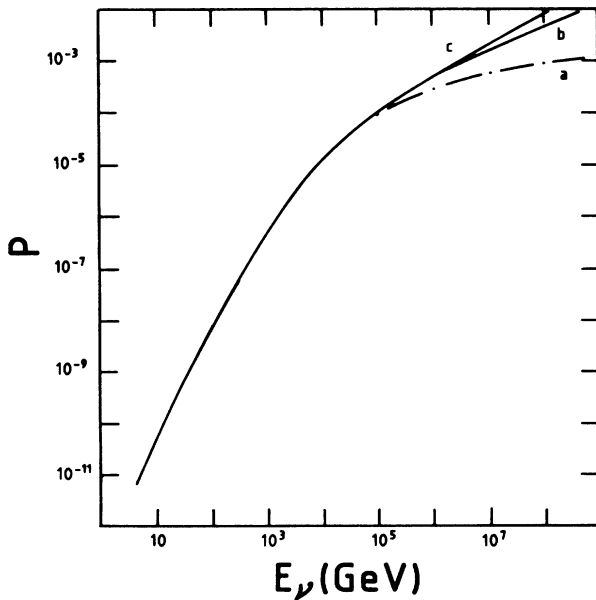


FIG. 2. Plot of $P(E_v)$. (a) and (b) as above, (c) is derived from fit 2 of Ref. 10.
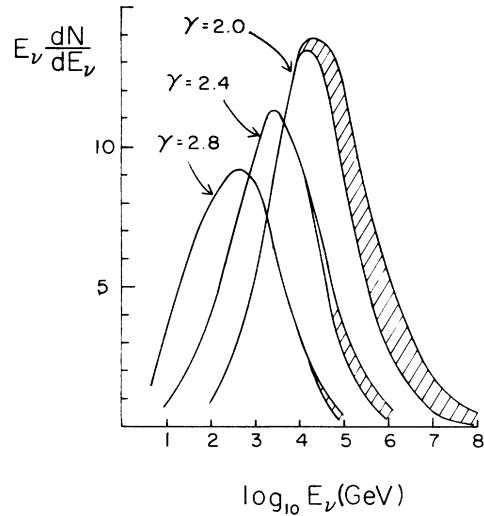


FIG. 3. Distribution of primary neutrino energies that give rise to upward muons with $E_\mu > 2$ GeV at the detector for power-law neutrino spectra with differential index $\gamma = 2.0$, 2.4, 2.8. The shaded region shows the difference between scaling and QCD-evolved structure functions.

It is easy to understand these results semiquantitatively from Eqs. (7)–(9) and Fig. 3. Neutrino interactions will be distributed uniformly from the detector out to the maximum range of the muon for a given neutrino energy $E_v \gtrsim E_\mu''$. From Eq. (9) the median range is thus

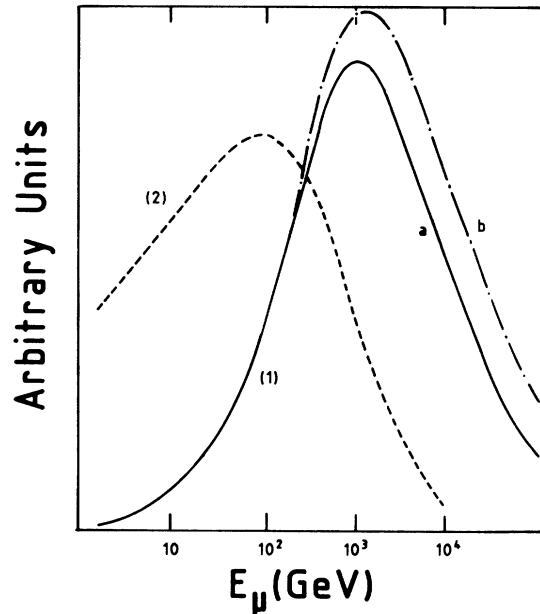$$X_M \lesssim \frac{1}{2\beta} \ln(1 + E_v/\epsilon) \quad \text{because } E_\mu'' \lesssim E_v \quad .$$



FIG. 4. Muon distribution $(dN_\mu/d \ln E_\mu)$ at the detector for neutrino spectrum $dN/dE_v \propto E^{-\gamma}$. (a) and (b) as above. (1) $\gamma = 2$, (2) $\gamma = 2.8$. Note that below $\gamma = 2.6$ (a) and (b) are practically the same.
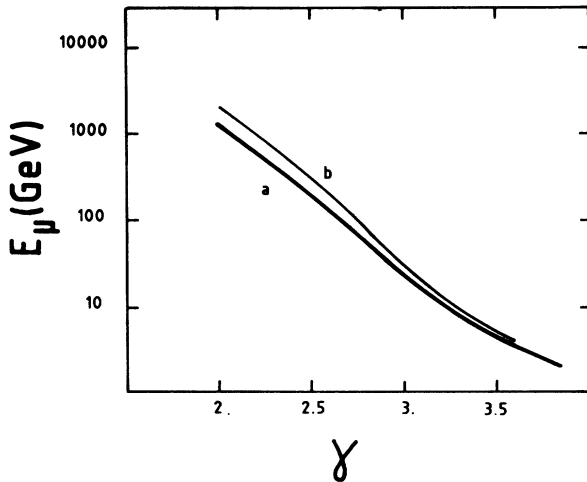
FIG. 5. Median muon energy at the detector vs $\gamma$.

The corresponding estimate of the median muon energy at the detector is

$$E_M \lesssim [\epsilon(\epsilon + E_\nu)]^{1/2} - \epsilon \ .$$

Numerically this gives $E_M \lesssim 1.8$ TeV for $E_\nu \simeq 10$ TeV.

## V. DISCUSSION

Hard neutrino spectra from energetic point sources are expected on two grounds. First, observation of air showers from point sources seem to indicate flat $\gamma$ spectra.[12] If neutrinos are produced in the same processes that produce the progenitors of the air showers, they would also have hard spectra. Second, the first-order Fermi acceleration mechanism in a strong shock accelerates protons with a power-law spectrum $dN/dE \propto E^{-\gamma}$ with $\gamma \gtrsim 2$ (Ref. 13). Such a mechanism could be effective in an accretion shock in an interacting x-ray binary[14] or in the termination shock in a pulsar wind model of a young supernova remnant.[15] Neutrinos produced by collisions of the accelerated protons would have similar spectra.[16,17]

In Fig. 6 we show the muon spectra expected at the detector for several neutrino spectra[16] consistent with reported air-shower observations of Cygnus X-3. For comparison we show the correctly normalized background of upward muons induced by atmospheric neutrinos. We conclude that a crude measure of muon energy (e.g., whether or not the muon is accompanied by a
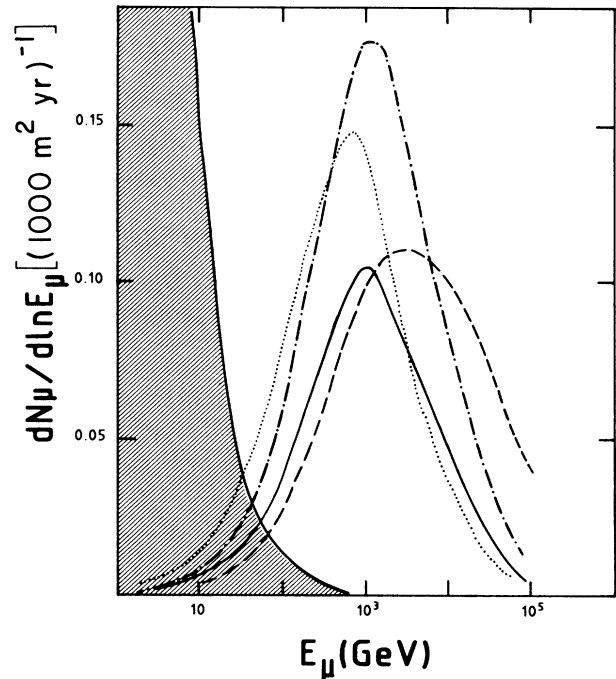


FIG. 6. Muon signal from Cygnus X-3 in different hypotheses Ref. 16: (1) ($\cdot \cdot \cdot \cdot$) proton spectrum $dN_p/dE_p \propto E_p^{-2}$, 2.8 $M_\odot$ companion; (2) (———) monoenergetic spectrum, $E_p = 10^8$ GeV, 2.8 $M_\odot$ companion; (3) (—·—·—·) 1000 g/cm$^2$ slab, $\rho = 10^{-7}$ g/cm$^3$, (4) (— — —) 1000 g/cm$^2$ slab, $\rho = 10^{-9}$ g/cm$^3$. Shaded area is the contribution of atmospheric neutrinos within the angular resolution for a point source.

shower in the detector) can easily distinguish a hard neutrino source from atmospheric background. It would, however, be difficult to distinguish among specific models of source spectra such as the ones illustrated in Fig. 6. If we take as a criterion $E_M > \epsilon \simeq 500$ GeV, inspection of Fig. 5 suggests that neutrino spectra with an equivalent $\gamma \lesssim 2.3$ should be distinguishable from softer spectra by a crude measurement of neutrino energies at the detector.

[1]M. F. Crouch et al., Phys. Rev. D **18**, 2239 (1978); M. R. Krishnaswamy et al., Pramana **19**, 525 (1982); M. M. Boliev et al., in Proceedings of the 17th International Cosmic Ray Conference, Paris, France, 1981 (Centre d'Etudes Nucleaires, Saclay, France, 1981), Vol. 7, p. 106; R. Svoboda et al., Astrophys. J. **315**, 420 (1987).

[2]R. Cowsik, Yash Pal, and S. N. Tandon, Proc. Indian Acad.

Sci. **53**, 217 (1966).

[3]T. K. Gaisser and Todor Stanev, Phys. Rev. D **30**, 985 (1984).

[4]G. L. Cassiday, Annu. Rev. Nucl. Part. Sci. **35**, 321 (1985).

[5]T. K. Gaisser and Todor Stanev, Phys. Rev. D **31**, 2770 (1985).

[6]V. S. Berezinsky and A. Z. Gazizov, Yad. Fiz. **29**, 1589 (1979) [Sov. J. Nucl. Phys. **29**, 816 (1980)].

[7]D. W. McKay and J. P. Ralston, Phys. Lett. **167B**, 103 (1986).

[8]C. Quigg, M. H. Reno, and T. P. Walker, Phys. Rev. Lett. **57**, 774 (1986).

[9]T. K. Gaisser and A. F. Grillo, Report No. LNF-86/27(P), 1986 (unpublished).

[10]D. W. Duke and J. F. Owens, Phys. Rev. D **30**, 49 (1984).

[11]L. V. Gribov, E. M. Levin, and M. G. Ryskin, Phys. Rep. **100**, 1 (1983).

[12]A. A. Watson, in *Proceedings of the 19th International Cosmic Ray Conference,* La Jolla, California, 1985, edited by F. C. Jones, J. Adams, and G. M. Mason (NASA Conf. Publ. 2376) (Goddard Space Flight Center, Greenbelt, MD, 1985), Vol. 9, p. iii.

[13]W. I. Axford, in *Proceedings of the 17th International Cosmic Ray Conference* (Ref. 1).

[14]D. Kazanas and D. C. Ellison, Nature (London) **319**, 380 (1986).

[15]T. K. Gaisser, A. K. Harding, and Todor Stanev, Nature (to be published).

[16]T. K. Gaisser and Todor Stanev, Phys. Rev. Lett. **54**, 2265 (1985). See, also, E. W. Kolb, M. S. Turner, and T. P. Walker, Phys. Rev. D **32**, 1145 (1985); **33**, 859(E) (1986); V. S. Berezinsky, C. Castagnoli, and P. Galleoti, Nuovo Cimento **8C**, 185 (1985).

[17]T. K. Gaisser and Todor Stanev, Phys. Rev. Lett. **58**, 1695 (1987); **59**, 844(E) (1987).